ESC European Society of Cardiology

Cardiovascular Research (2022) **118**, 2703–2717
https://doi.org/10.1093/cvr/cvab304

# Role of PDE10A in vascular smooth muscle cell hyperplasia and pathological vascular remodelling

**Lingfeng Luo [1,2], Yujun Cai[2], Yishuai Zhang [2], Chia G. Hsu [2], Vyacheslav A. Korshunov[2], Xiaochun Long[3], Peter A. Knight[4], Bradford C. Berk [2], and Chen Yan [2]***

[1]Department of Biochemistry and Biophysics, University of Rochester School of Medicine and Dentistry, Rochester, NY, USA; [2]Department of Medicine, Aab Cardiovascular Research Institute, University of Rochester School of Medicine and Dentistry, Rochester, NY, USA; [3]Department of Vascular Biology Center and Medicine, Medical College of Georgia, Augusta, GA, USA; and [4]Department of Surgery, University of Rochester School of Medicine and Dentistry, Rochester, NY, USA

*Received 14 September 2020; editorial decision 12 September 2021; accepted 17 September 2021; online publish-ahead-of-print 22 September 2021*

**Time for primary review: 33 days.**

**Aims** Intimal hyperplasia is a common feature of vascular remodelling disorders. Accumulation of synthetic smooth muscle cell (SMC)-like cells is the main underlying cause. Current therapeutic approaches including drug-eluting stents are not perfect due to the toxicity on endothelial cells and novel therapeutic strategies are needed. Our preliminary screening for dysregulated cyclic nucleotide phosphodiesterases (PDEs) in growing SMCs revealed the alteration of PDE10A expression. Herein, we investigated the function of PDE10A in SMC proliferation and intimal hyperplasia both *in vitro and in vivo*.

**Methods and results** RT-qPCR, immunoblot, and *in situ* proximity ligation assay were performed to determine PDE10A expression in synthetic SMCs and injured vessels. We found that PDE10A mRNA and/or protein levels are up-regulated in cultured SMCs upon growth stimulation, as well as in intimal cells in injured mouse femoral arteries. To determine the cellular functions of PDE10A, we focused on its role in SMC proliferation. The anti-mitogenic effects of PDE10A on SMCs were evaluated via cell counting, BrdU incorporation, and flow cytometry. We found that PDE10A deficiency or inhibition arrested the SMC cell cycle at G1-phase with a reduction of cyclin D1. The anti-mitotic effect of PDE10A inhibition was dependent on cGMP-dependent protein kinase Iα (PKGIα), involving C-natriuretic peptide (CNP) and particulate guanylate cyclase natriuretic peptide receptor 2 (NPR2). In addition, the effects of genetic depletion and pharmacological inhibition of PDE10A on neointimal formation were examined in a mouse model of femoral artery wire injury. Both PDE10A knockout and inhibition decreased injury-induced intimal thickening in femoral arteries by at least 50%. Moreover, PDE10A inhibition decreased *ex vivo* remodelling of cultured human saphenous vein segments.

**Conclusions** Our findings indicate that PDE10A contributes to SMC proliferation and intimal hyperplasia at least partially via antagonizing CNP/NPR2/cGMP/PKG1α signalling and suggest that PDE10A may be a novel drug target for treating vascular occlusive disease.

*Corresponding author. Tel: 585-276-7704, E-mail: chen_yan@urmc.rochester.edu

**Graphical Abstract**

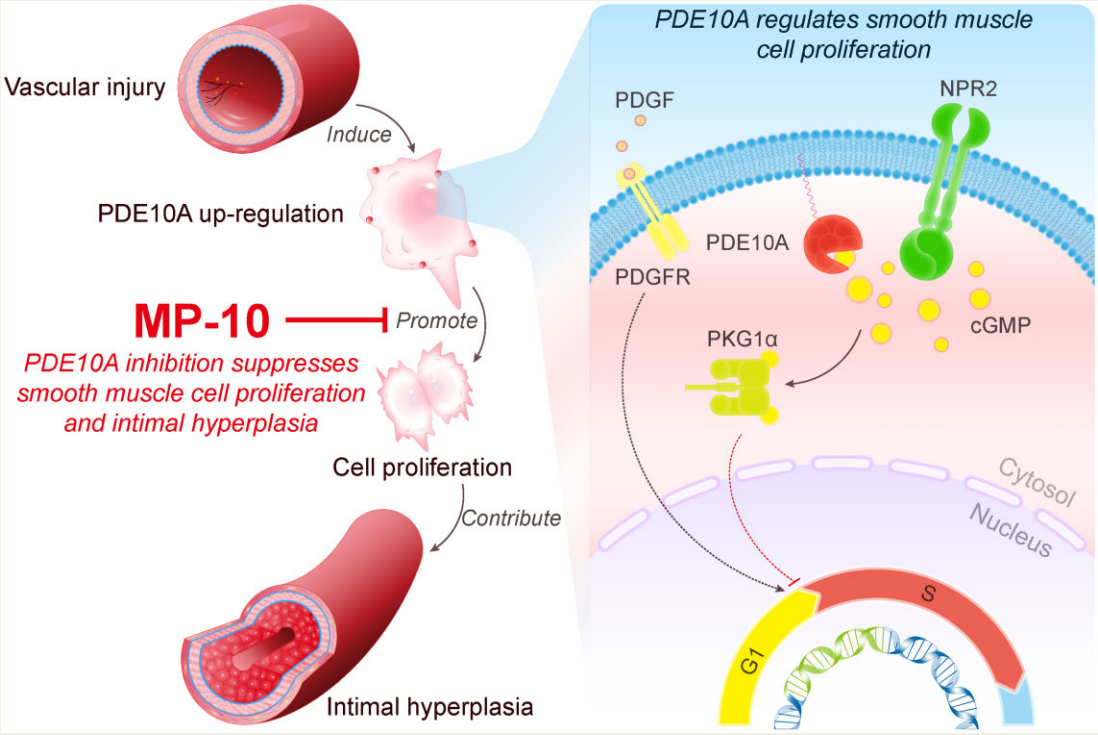


**Keywords** Phosphodiesterase • Smooth muscle cell • SMC • Neointima • cGMP

# 1. Introduction

Intimal hyperplasia (also referred to as neointimal hyperplasia) characterized by thickening of the tunica intima of a blood vessel, is a common feature of vascular remodelling disorders such as post-angioplasty restenosis,[1,2] bypass graft stenosis,[3] and accelerated atherosclerosis.[4,5] It contributes to gradually narrowed vessel lumen, reduced blood flow, and eventually ischaemia. Activation and subendothelial accumulation of smooth muscle cell (SMC)-like cells are the main underlying cause of intimal hyperplasia.[6] Unlike normal quiescent SMCs (known as contractile SMCs) that reside in the media layer of healthy vessel walls, these activated and proliferative SMCs are called synthetic SMCs.[7] They form a new layer between the lumen and the internal elastic lamina, which is often called the neointima. The proliferation of SMCs under stimulation by growth factors and cytokines in response to vascular injury can contribute to 90% of the ultimate intima proliferation.[8] Current therapeutic approaches including commonly used drug-eluting stents targeting cell growth still have issues such as in-stent stenosis and delayed re-endothelialization,[9–11] especially among high-risk patients.[12] Therefore, more effective therapeutic strategies are still in urgent demand.

Though cyclic nucleotide-dependent signalling pathways are well known for maintaining the vascular tone and regulating the contraction and relaxation of SMCs,[13] they also take part in synthetic SMC proliferation and neointimal formation under pathological conditions.[14–16] Previous studies have shown that cAMP or cGMP regulates SMC growth by activating the direct downstream effectors of cyclic nucleotide signalling such as cAMP-dependent protein kinase (PKA)[15] and cGMP-dependent protein kinase (PKG).[17] The cyclic nucleotide phosphodiesterase (PDE) superfamily plays a pivotal role in modulating cyclic nucleotide signalling as a fine tuner. Among all 11 PDE protein families, PDE1,[18] PDE3,[19] PDE4,[20] and PDE5[21] have been reported to regulate SMC proliferation and vascular remodelling. A number of PDE family-specific inhibitors have been in clinical trials or clinical uses for treating other diseases[22]; thus research on the functions of PDEs in vascular pathophysiology may lead to novel applications of these inhibitors in vascular disorders.

PDE10A is the single member of PDE10 protein family, and it catalyzes both cAMP and cGMP hydrolysis. The literature on PDE10A has been focused on psychiatric and neurological disorders[23–25] because PDE10A[26] expression is enriched in the striatal region of the brain under normal conditions.[27–30] Interestingly, PDE10A expression is up-regulated in a number of pathological conditions, which plays a causative role in the pathogenesis of the diseases. For example, PDE10A expression was increased in several cancer cells such as colorectal[31] and non-small cell lung cancer cells.[32] Inhibition of PDE10A suppressed growth of these tumour cells *in vitro*. We have recently shown that PDE10A expression is significantly increased in human and mouse failing hearts.[33] Genetic ablation or pharmacological inhibition of PDE10A significantly attenuated pathological cardiac remodelling and dysfunction induced by chronic pressure overload or neurohormonal stimulation, suggesting a

critical role of PDE10A up-regulation in related cardiac diseases.[33] To understand how individual PDE isozymes contribute to SMC pathogenesis in vascular remodelling, we performed preliminary studies to find PDEs whose expression increased in proliferative SMCs. We identified PDE10A as one of the PDEs significantly up-regulated in growing SMCs. In the current study, we aimed to determine the role of PDE10A in synthetic SMCs *in vitro*, in a mouse model of vascular remodelling *in vivo*, as well as human saphenous vein (HSV) remodelling *ex vivo*. In addition, we characterized the mechanistic action of PDE10A on synthetic SMC growth.

# 2. Materials and methods

Expanded methods are available in the Supplementary material online.

## 2.1 Femoral artery wire injury model

Animal husbandry and all surgical procedures are in accordance with the guidelines of the University Committee on Animal Resources (UCAR) at the University of Rochester, and in compliance with the 'Principles of Laboratory Animal Care' (NIH publication No. 85-23, revised 1985) and the 'Guide for the Care and Use of Laboratory Animals' (8th edition, National Academies Press, Washington, DC, USA, 2011). The PDE10A knockout and wild-type mice were all home bred, while the mice used for MP-10 administration was purchased from the Jackson lab. To compare PDE10A knockout and wild-type mice, 12 weeks old male or female littermates on a C57BL/6 background were chosen. The femoral artery wire injury was performed as previously described. Mice were anaesthetized by inhalation of 2% isoflurane. The left common femoral artery and its branches were dissected under a dissecting microscope. The femoral artery is looped proximally with 6-0 nylon suture and the branches were looped distally. Then a transverse arteriotomy was performed on the muscular branch, followed by insertion of a spring wire (0.38 mm in diameter, C-SF-15-15, COOK) towards the iliac artery. The wire was left inside for 1 min before being retrieved. The muscular branch was ligated at the point of bifurcation with 8-0 silk suture. The blood flow was restored and the skin incision was closed. Four weeks after surgery, mice were anaesthetized by intraperitoneal injection of a cocktail of ketamine (80 mg/kg) and midazolam (0.6 mg/kg), and perfused with saline. Then mice were perfused with 10% neutral buffered formalin (10% NBF) and undergone cervical dislocation as the final euthanasia method. The sham and injured femoral arteries were fixed in 10% NBF overnight and then embedded in paraffin. Cross-sections were obtained. To examine MP-10 treatment, 12 weeks old male C57BL/6 mice were randomly assigned into two groups. The experiment group was treated with MP-10 (10 mg/kg/day) in 40% (w/v in saline) 2-hydroxypropyl-β-cyclodextrin (HP-β-CD) subcutaneously, and the control group with the vehicle HP-β-CD alone. The MP-10 we used was shared by Pfizer Inc. in this animal model. The treatment started 3 days before the injury and continued for 4 weeks post-injury. Other mice not subjected to tissue harvesting were euthanized by carbon dioxide inhalation and cervical dislocation.

## 2.2 Proximity ligation assay

Proximity ligation assay (PLA) is a method to detect proteins in proximity. Two primary PDE10A antibodies (Santa Cruz, sc-515023 and Novus Biologicals, NB300-645) raised in mice and rabbits that recognize different epitopes of the PDE10A protein were used. Two PLA probes as secondary antibodies were conjugated to specific single-stranded oligonucleotides. Then the signal was amplified by rolling DNA polymerization, which was followed by hybridization with fluorescent-labelled complementary oligonucleotide probes. The Duolink™ In Situ Red Starter Kit Mouse/Rabbit (DUO92101, Sigma-Aldrich) was used. Paraffin-embedded tissue sections were deparaffinized and rehydrated. Tissue antigen retrieval was conducted with citric acid buffer. Then samples were blocked and incubated with primary antibodies. Samples were washed in wash buffer A and incubated with PLA probes. Then samples were washed again in wash buffer A and incubated with the ligase and ligase buffer. After being washed in buffer A and incubated with the polymerase and rolling circle amplification buffer for 100 min at 37°C, samples were washed in wash buffer B and mounted with a mounting solution containing DAPI.

## 2.3 Cell growth assay

Rat aortic SMCs between passages 10–15 were used throughout the whole study. These SMCs were originally purchased commercially. Experiments were carried out with these cells at different times in at least three independent experiments. Cells were cultured in Dulbecco's modified Eagle's medium (DMEM) medium containing 10% foetal bovine serum (FBS) and 1% 100 U/mL penicillin/streptomycin. For testing PDE10A inhibition, cells were serum-deprived for 2 days, pretreated with vehicle or MP-10 for 30 min, and then stimulated with 2% FBS for 2 days. Then cell numbers were counted. For examining PDE10A shRNAs, rat SMCs were transduced with lentiviruses carrying control or PDE10A shRNAs and serum-starved for 3 days, followed by 2% FBS stimulation for 2 days. The MP-10 used in *in vitro* assays was purchased from Selleckchem (S1032).

## 2.4 BrdU incorporation assay

Cells were serum-deprived and pretreated with MP-10 or shRNAs as above. After starvation and pretreatment, cells were stimulated by 2% FBS with 10 μM BrdU for 24 h. Then cells were fixed by 4% paraformaldehyde and immunostained for BrdU (ab74545, Abcam) and DAPI. The percentage of BrdU positive cells was counted.

## 2.5 TUNEL assay

Cells were serum-starved for 2 days and pretreated with vehicle or MP-10 for 30 min. Cells were stimulated with 2% FBS for 14 h. $H_2O_2$ was added as a positive control. Then cells were stained with *in situ* cell death detection kit (12156792910, Roche). Briefly, cells were fixed, permeabilized, and incubated with TUNEL reaction mixture.

## 2.6 Propidium iodide staining and flow cytometry

The staining was performed following the instructions of the propidium iodide flow cytometry kit (ab139418, Abcam). Briefly, cells were harvested in single-cell suspension and fixed in 66% ethanol. After being rehydrated in PBS, cells were stained with 0.05 mg/mL propidium iodide and 550 U/mL RNase for 30 min. Then cells were analysed by a flow cytometer with 488 nM laser excitation.

## 2.7 HSV *ex vivo* culture

HSV discards after coronary artery bypass graft (CABG) surgery were collected from Strong Memorial Hospital (Rochester, NY, USA). They are exempted from human subject restrictions by Research Subjects Review Board (RSRB) at the University of Rochester Medical Center. The study was carried out in accordance with the principles outlined in the Declaration of Helsinki. The HSV segments were cultured as

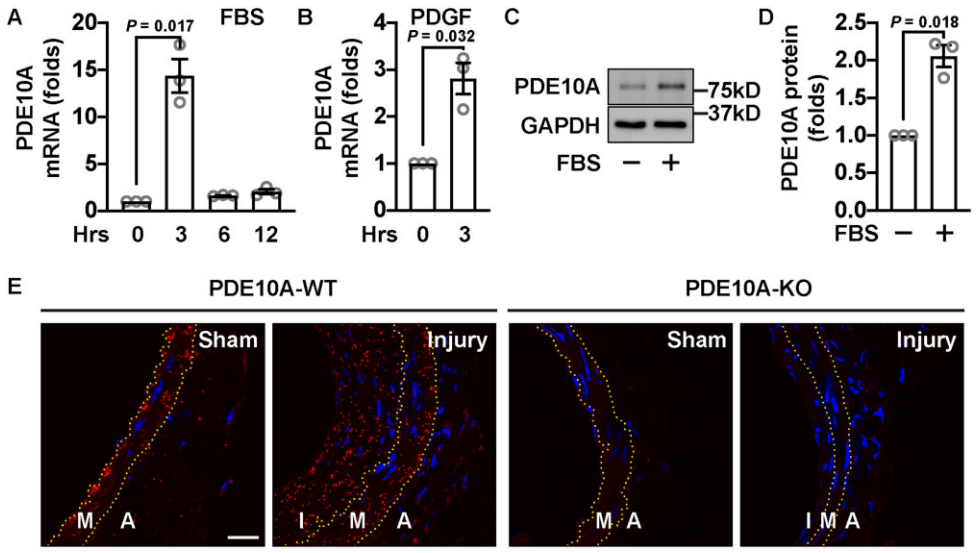


**Figure 1** PDE10A expression level is increased in growing SMCs *in vitro* and SMC-like cells in intimal lesions *in vivo*. (*A*) RT-qPCR results showing relative PDE10A mRNA levels in rat SMCs stimulated with FBS for different amounts of time. Cells were starved for 2 days before being treated with 10% FBS. $n = 3$ for each group. A one-sample *t*-test was performed to determine the significance of the fold change. (*B*) RT-qPCR results showing PDGF-induced PDE10A expression in rat SMCs. Cells were serum-deprived for 2 days and then treated with 10 ng/mL PDGF-BB for 3 h. A one-sample *t*-test was conducted. $n = 3$ for each group. (*C*) Immunoblots showing PDE10A and GAPDH levels of rat SMCs with FBS stimulation. Cells were starved for 2 days and then incubated with 10% FBS for 6 h. (*D*) Quantitative results of (*C*). $n = 3$ for each group. The signal of PDE10A bands was first normalized to the input and then normalized to the group without FBS treatment. A one-sample *t*-test was performed. $n = 3$ for each group. (*E*) Representative images of the proximity ligation assay on PDE10A expression in cross-sections of wire-injured mouse femoral arteries. The left femoral arteries were injured and the right femoral arteries served as sham controls. Femoral arteries were harvested 4 weeks after the surgery. Yellow dash lines indicate the internal and external elastic laminae. A, adventitia; I, intima; M, media. Similar observations were obtained from tissue samples from at least three different mice. Scale bar = 20μm. All data are shown as mean ± SEM.

previously described with some modifications. The segments were opened longitudinally and cut transversely into 0.5 cm lengths. Each piece was pinned on a piece of surgical mesh and cultured with its luminal surface facing up in a well of 12-well plates with RPMI 1640 medium containing 15% FBS with vehicle (DMSO) or 20 μM MP-10. The medium and MP-10 were replaced every other day. After 2 weeks, samples were washed, fixed in 10% NBF overnight, and embedded in paraffin.

## 2.8 Statistical analysis

All data are presented as mean ± standard error of the mean. Statistical analysis was performed using GraphPad Prism 8 software. The D'Augostino and Pearson omnibus normality test were used to test the normality of *in vivo and ex vivo* data. The Shaprio–Wilk normality test was adopted for *in vitro* data including these with $n = 3$/group. If the data followed a normal distribution, a parametric test was carried out, but with a Welch's correction if the variance is unequal; otherwise, a nonparametric test was performed. For comparison of normalized data to the reference, a one-sample Student's *t*-test was performed. To compare two data groups, a Student's unpaired *t*-test was used for a parametric test or a Mann–Whitney *U* test was performed for a nonparametric test. When it came to three or more groups, a one-way analysis of variance (ANOVA) followed by Bonferroni's *post hoc* test or a Welch's ANOVA with Dunnett's T3 multiple comparison test was used for a parametric test, or a Kruskal–Wallis test with Dunn multiple comparisons was conducted for a non-parametric test.

# 3. Results

## 3.1 PDE10A expression is up-regulated by serum or PDGF in cultured rat SMCs

We first examined changes in PDE10A expression when cultured SMCs were treated with mitogenic stimuli such as serum or platelet-derived growth factor (PDGF)-BB. Rat SMCs were starved for 2 days and then incubated with FBS for different times. We found that PDE10A mRNA was up-regulated by FBS with a peak at 3 h (*Figure 1A*). Consistently, PDE10A mRNA up-regulation was also observed in SMCs stimulated by PDGF-BB (*Figure 1B*). Consistent with the increase in mRNA expression, PDE10A protein expression also increased (*Figure 1C and D*). We also found that the PDE10A level was low in various types of contractile vascular SMCs but was largely enhanced in corresponding growing/synthetic SMCs (Supplementary material online, *Figure S1*). Due to the nonspecific issues of the currently available PDE10A antibodies in immunostaining of vascular tissues, we performed *in situ* PLAs to detect PDE10A proteins with two different PDE10A antibodies. We found that PDE10A protein expression was significantly increased in the intima and media areas of wire-injured mouse femoral arteries compared to the control

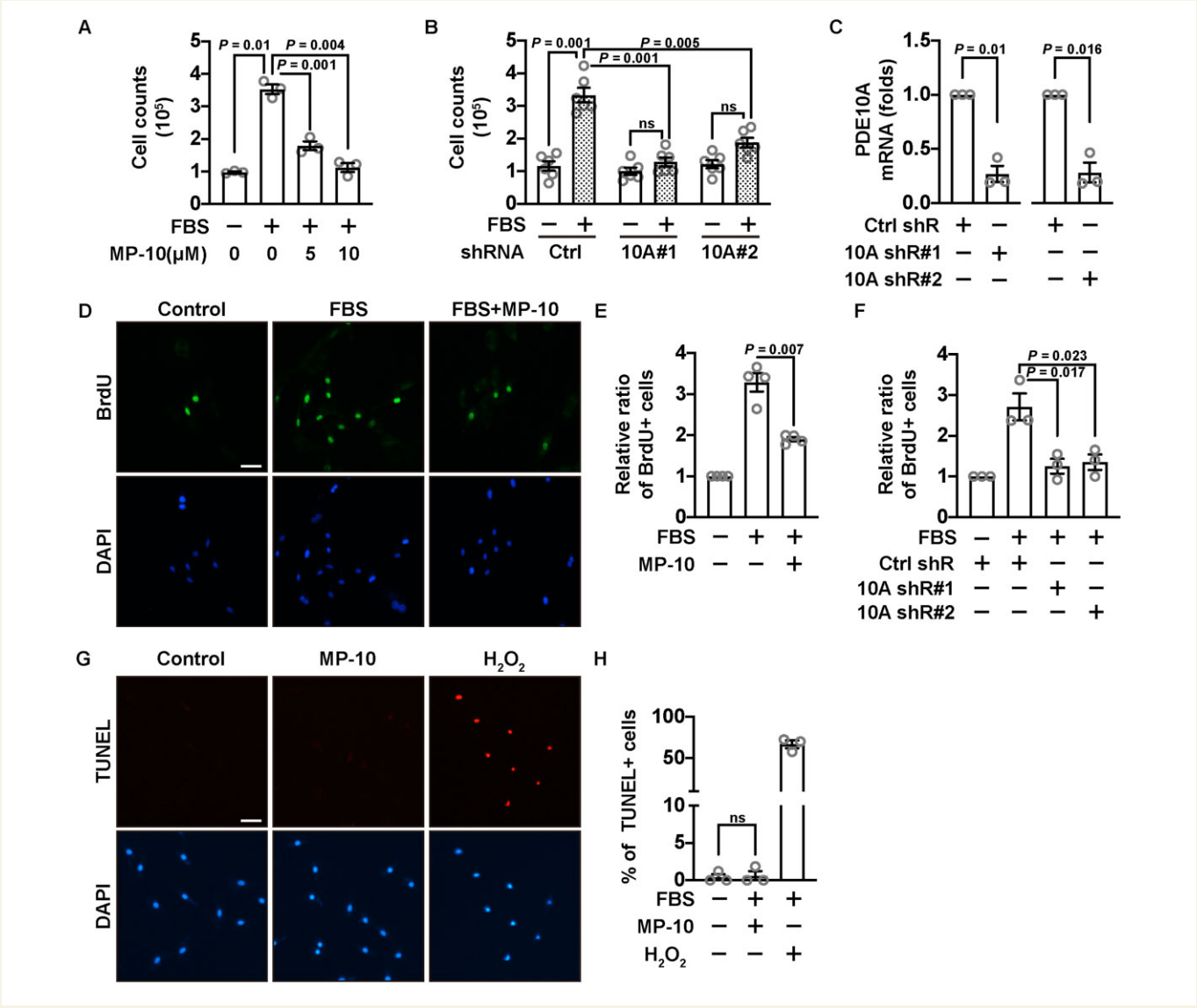


**Figure 2** The effects of PDE10A inhibition or knocking down on SMC proliferation or death. (*A*) Cell numbers of rat SMCs after being starved for 2 days and then stimulated by 2% FBS in the presence of different doses of MP-10. A Welch's ANOVA with Dunnett's T3 multiple comparisons test was performed. $n = 3$ for each group. (*B*) Cell numbers of rat SMCs with PDE10A knockdown by two different pairs of shRNAs, after being starved and stimulated with FBS. Cells were treated with lentivirus-mediated shRNAs 3 days before FBS stimulation. A Welch's ANOVA with Dunnett's T3 multiple comparisons test was carried out. $n = 6$ for each group. (*C*) RT-qPCR results showing the efficiency of PDE10A knockdown. The expression level of PDE10A was normalized to the control shRNA group. One-sample *t*-tests were performed. $n = 3$ for each group. (*D*) Representative immunofluorescent images of BrdU positive rat SMCs treated with vehicle or MP-10 (5 μM). Cells were starved for 2 days and then stimulated by 2% FBS. (*E*) Quantitative data showing relative ratios of BrdU positive SMCs. The ratios were normalized to the group without FBS stimulation. An unpaired Student's *t*-test with Welch's correction was conducted to compare the FBS-stimulated proliferation without and with MP-10. $n = 4$ for each group. (*F*) Relative ratios of BrdU positive SMCs after PDE10A silencing by shRNAs. A one-way ANOVA with Bonferroni's multiple comparisons test was applied. $n = 3$ for each group. (*G*) Representative images of TUNEL staining of rat SMCs after 5 μM MP-10 treatment. Red signals indicate apoptotic cells. $H_2O_2$ was used as a positive control. (*H*) Quantitative data of the TUNEL staining in (*G*). The percentages of TUNEL positive cells against DAPI (total cells) were calculated. A Kruskal–Wallis test was performed. $n = 3$ for each group. Scale bar = 50μm. All data are shown as mean ± SEM. ns, not significant.

ones (*Figure 1E*, left panels). The staining specificity was confirmed in femoral arteries from PDE10A knockout (PDE10A-KO) mice (*Figure 1E*, right panels) and in negative controls treated with each primary antibody alone (Supplementary material online, *Figure S2*).

## 3.2 PDE10A inhibition reduces synthetic SMC proliferation but does not trigger significant cell death

To determine whether PDE10A directly regulates SMC growth, we performed cell growth assays by inhibiting PDE10A activity with a PDE10A-

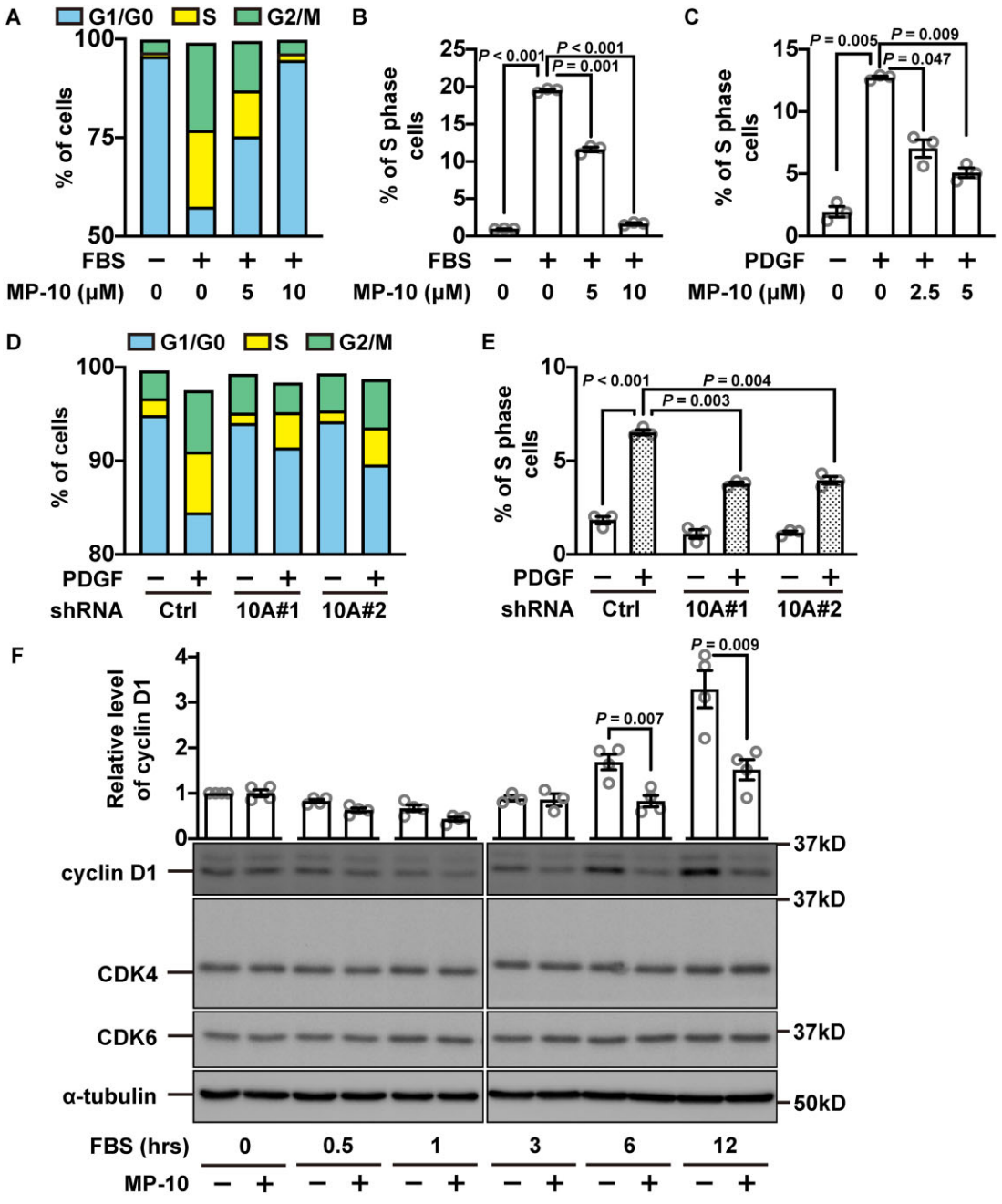


**Figure 3** Cell cycle arrest of SMCs induced by PDE10A inhibition or silencing. (*A*) Percentages of rat SMCs in different phases of a cell cycle after being treated with MP-10. Rat SMCs were starved for 2 days, followed by 2% FBS stimulation. The blue boxes indicate cells in the G1/G0 phase, the yellow boxes show cells in the S phase and the green colour is for cells in the G2/M phase. (*B*) Percentages of S-phase cells after being treated with MP-10 in addition to FBS. A Welch's ANOVA with Dunnett's T3 multiple comparisons test was performed. $n = 3$ for each group. (*C*) Percentages of S-phase cells after being stimulated by PDGF (10 ng/mL) and treated with MP-10. A Welch's ANOVA with Dunnett's T3 multiple comparisons test was conducted. $n = 3$ for each group. The percentages of cells in (*D*) all phases or in (*E*) S-phase alone after cells being knocked down of PDE10A and stimulated via 10 ng/mL PDGF. Cells were transduced by lentiviruses expressing different PDE10A shRNAs 3 days before PDGF stimulation. A Welch's ANOVA with Dunnett's T3 multiple comparisons test was implemented. $n = 3$ for each group. (*F*) Western blot showing the expression of cyclin D1 at different time points after SMCs were starved and then stimulated by 2% FBS with vehicle or 5 μM MP-10. The upper part shows the relative quantification results, while the lower part exhibits the representative images of immunoblot staining of cyclin D1, CDK4, CDK6, and α-tubulin. Unpaired Student's *t*-tests were conducted on comparison within each time point. $n = 3$–4 for each group. All data are shown as mean ± SEM.

selective inhibitor, MP-10 (Mardepodect, PF-2545920), or by knocking down PDE10A mRNA with lentivirus-mediated expression of PDE10A shRNAs. In a cell number counting assay, we found that MP-10 was capable of dose-dependently suppressing the increase of SMC numbers after FBS stimulation (*Figure 2A*). MP-10 alone without FBS did not significantly affect SMC growth (data not shown). Two different pairs of PDE10A shRNAs also decreased SMC numbers (*Figure 2B*) with a knockdown efficiency of roughly 75% (*Figure 2C* and Supplementary material online, *Figure S3A*). Next, we performed the BrdU incorporation assay that is widely used to study cellular proliferation, as BrdU (a thymidine analogue) can be incorporated into DNA of actively dividing cells. We observed that MP-10 significantly reduced the percentage of BrdU positive cells (*Figure 2D and E*), as did PDE10A shRNAs (*Figure 2F*). Similar anti-proliferative effects of MP-10 were also observed in cultured human coronary artery SMCs, human aortic SMCs, HSV SMCs, and mouse aortic SMCs (Supplementary material online, *Figure S4*). Surprisingly, MP-10 did not cause severe cell death as shown by the TUNEL (*Figure 2G and H*) or trypan blue staining (Supplementary material online, *Figure S5*). Additionally, we examined the effects of PDE10A deficiency on SMC migration by the scratch wound healing assay but only observed a mild decrease (roughly 15%) in migration with PDE10A shRNAs (data not shown). We thus focused on the role of PDE10A in SMC proliferation.

## 3.3 PDE10A inhibition arrests the cell cycle of SMCs at G1-phase with a reduction of cyclin D1

To further dissect the function of PDE10A in regulating SMC proliferation, we performed flow cytometry with propidium iodide staining, which measures the percentage of cells in each phase of a cell cycle: G1/G0, S, and G2/M phases. First, we synchronized the cell cycle by serum starvation and then stimulated cell growth with FBS in the presence of different doses of MP-10 (*Figure 3A*). We found that S-phase was the most affected phase due to MP-10 treatment (*Figure 3A*), and MP-10 dose-dependently decreased the percentage of S-phase cells (*Figure 3B*). A similar cell cycle inhibition was also observed when we switched to PDGF-BB, a key growth factor implicated in intimal hyperplasia (*Figure 3C*). Similarly, the cell cycle arrest was also observed in SMCs treated with PDE10A shRNAs (*Figure 3D and E*). Cyclin D1 is an essential protein for cell cycle progression from G1-phase to S-phase.[34] Upon MP-10 treatment, cyclin D1 expression was significantly diminished (*Figure 3F*). However, other cell cycle proteins such as Cdk4 and Cdk6 did not change significantly (*Figure 3F*).

## 3.4 PDE10A regulates SMC proliferation through cGMP/PKG1α signalling

PDE10A can hydrolyse both cAMP and cGMP.[27–30] We found that both cAMP and cGMP levels were elevated in SMCs by MP-10 (*Figure 4A and B*). The most well-known cAMP and cGMP effector molecules implicated in SMC growth are the PKA and PKG. We, therefore, examined the roles of PKA and PKG in the anti-mitotic effect of the PDE10A inhibitor MP-10. We found that the inhibitory effect of MP-10 on SMC proliferation was not significantly changed upon inhibiting PKA by PKI peptides (*Figure 4C*). However, a PKG inhibitor, DT-2, appeared to partially block the inhibitory effect of MP-10 on SMC proliferation (*Figure 4D*). PKG1 is the only PKG gene expressed in SMCs, but there are two PKG1 isoforms PKG1α and PKG1β generated by alternative splicing. The major difference between those two isoforms comes from the end of the N-terminal sequence, which may mediate their targeting to different subcellular compartments.[35] To functionally distinguish those two isoforms, we designed siRNA specifically targeting PKG1α or PKG1β (*Figure 4E and F* and Supplementary material online, *Figure S3B and C*). We found that PKG1α siRNA was able to abolish the inhibitory effect of MP-10 on SMC proliferation (*Figure 4G*), suggesting that PKG1α activation mediates the anti-proliferating effects of PDE10A inhibition. In contrast, we found that PKG1β siRNA itself elicited anti-proliferative effects (*Figure 4H*), suggesting PKG1β activation may promote SMC proliferation.

## 3.5 PDE10A-mediated regulation of SMC proliferation involves CNP and guanylate cyclase NPR2

There are two types of enzymes that synthesize cGMP in SMCs, soluble guanylate cyclases (sGCs) in the cytosol and particulate guanylate cyclases (pGCs) on the plasma membrane. Blocking sGCs with ODQ did not notably affect SMC proliferation (Supplementary material online, *Figure S6*). There are two types of natriuretic peptide receptors (NPR1 and NPR2) possessing intrinsic pGC activities. We found that the level of NPR2 was much higher than NPR1 in cultured SMCs (*Figure 5A*), thus we focused on NPR2. We found that the anti-proliferative effect of MP-10 was abolished under the condition when NPR2 was knocked down by an siRNA (*Figure 5B and C* and Supplementary material online, *Figure S3D*). It has been reported that the NPR2 ligand C-natriuretic peptide (CNP) is synthesized in synthetic SMCs and may act as an autacoid.[36,37] We, therefore, determined the role of SMC CNP by knocking down the synthesis of the CNP precursor (gene name *NPPC*) (*Figure 5D*). We found that NPPC siRNA suppressed the inhibitory effect of MP-10 on SMC proliferation (*Figure 5E*). In addition, MP-10 and CNP showed additive effects on SMC proliferation (*Figure 5F*).

To determine the potential interaction of PDE10A and NPR2, confocal microscopy and co-immunoprecipitation were performed. Overexpression of EGFP-tagged PDE10A2 isozyme (the major isoform in SMCs) and mCherry-tagged NPR2 in 293A cells or SMCs showed an overlap of the signals on the plasma membrane (*Figure 5G and H*). It has been reported that PDE10A2 is localized close to the cell membrane via palmitoylation.[38] The co-immunoprecipitation experiment showed that Flag-tagged PDE10A could be pulled down together with HA-tagged NPR2 in 293A cells (*Figure 5I*). These results suggest that PDE10A2 is localized proximately to NPR2 and negatively regulates CNP/NPR2/cGMP signalling.

## 3.6 PDE10A knockout ameliorates wire injury-induced intimal hyperplasia in mice

To determine whether PDE10A directly contributes to neointimal formation, we performed left femoral artery (LFA) wire injury in global PDE10A-KO mice compared to PDE10A wild-type (PDE10A-WT) control mice on the C57BL/6J background. This PDE10A-KO line has normal growth rates and feeding patterns, as well as normal nursing and mating behaviours.[39] The right femoral artery (RFA) was used as the sham control. Modified Verhoeff-van Gieson (VVG) staining was performed on cross-sections of paraffin-embedded femoral artery samples. The black-stained internal elastic lamina and external elastic lamina (EEL) define two anatomical boundaries between intima-media and media-adventitia (*Figure 6A*). The injured LFAs of PDE10A-WT mice developed a thick intimal layer between the lumen and the internal elastic lamina, while the sham RFAs had no visible layer of intima. However, in PDE10A-KO mice, intimal thickening was much less than in PDE10A-

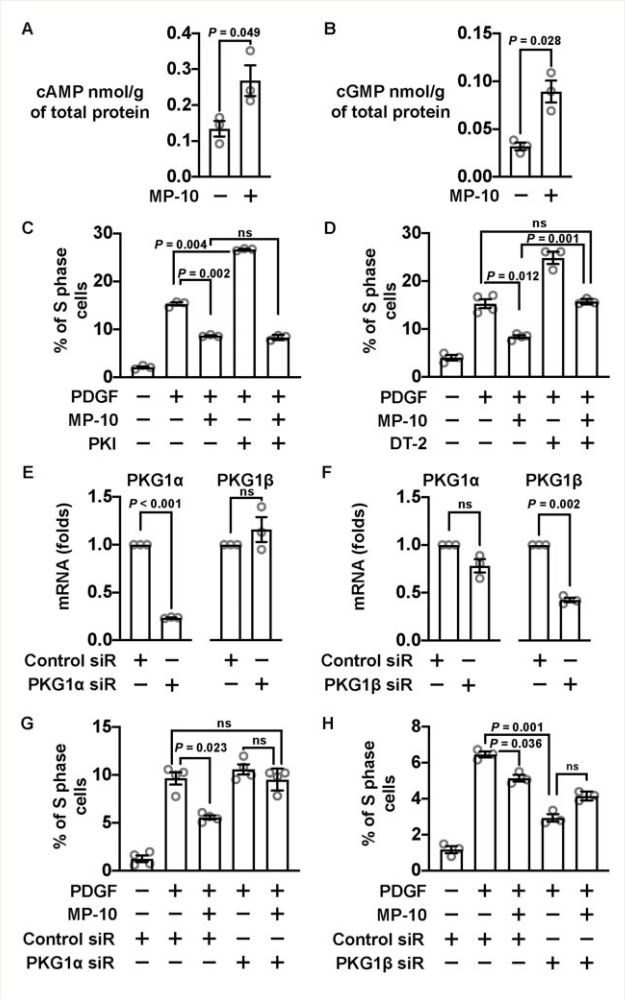


**Figure 4** PDE10A modulated SMC proliferation involves cGMP signalling pathway. (*A*) cAMP ELISA results showing the change of cAMP concentration after rat SMCs were treated with 5 μM MP-10. An unpaired Student's *t*-test was performed. $n = 3$ for each group. (*B*) cGMP concentration changes after MP-10 treatment revealed by cGMP ELISA. An unpaired Student's *t*-test with Welch's correction was conducted. $n = 3$ for each group. (*C*) Percentages of S-phase cells after being stimulated by 10 ng/mL PDGF and treated with 2.5 μM MP-10 and 10 μM PKI (a PKA inhibitor). Cells were starved for 2 days before PDGF stimulation. A Welch's ANOVA with Dunnett's T3 multiple comparison test was performed to determine the effects of MP-10 and PKI on SMC proliferation. $n = 3$ for each group. (*D*) Percentages of S-phase cells treated with 2.5 μM MP-10 and 5 μM DT-2 (a PKG inhibitor). A Welch's ANOVA with Dunnett's T3 multiple comparisons test was applied. $n = 3$–4 for each group. (*E*) RT-qPCR results showing the mRNA levels of PKG1α and PKG1β after knocking down PKG1α in rat SMCs. The expression levels were normalized to negative control siRNA groups. One-sample *t*-tests were performed to determine the knockdown efficiency. $n = 3$ for each group. (*F*) RT-qPCR results showing the levels of PKG1α and PKG1β after PKG1β silencing. One-sample *t*-tests were conducted. $n = 3$ for each group. (***G***) Percentages of S-phase cells treated with control or PKG1α siRNA and 2.5 μM MP-10. A Welch's ANOVA with Dunnett's T3 multiple comparisons test was applied. $n = 4$ for each group. (*H*) Percentages of S-phase cells treated with PKG1β siRNA and 2.5 μM MP-10. A Welch's ANOVA with Dunnett's T3 multiple comparisons test was applied. $n = 3$ for each group. All data are shown as mean ± SEM. ns, not significant.

WT mice. The quantitative results from the average of 5 LFA cross-sections at 300 μm intervals from each animal revealed a significantly reduced intimal area (*Figure 6B*), an unaffected medial area (*Figure 6C*), and a decreased ratio of intima/media (*Figure 2D*) in male PDE10A-KO mice compared to male PDE10-WT mice. We obtained similar results between PDE10A-WT and PDE10A-KO female mice (*Figure 2E–G*). We did not observe significant differences in the length of the EEL between injured femoral arteries of male WT and KO mice (Supplementary material online, *Figure S7A*). However, there was a slight decrease (~10%) in the EEL length between female WT and KO mice (Supplementary material online, *Figure S7B*). Interestingly, injured femoral arteries of both PDE10A-WT and PDE10A-KO mice showed similar full coverage of endothelial cells 4 weeks after the injury (data not shown).

## 3.7 PDE10A inhibitor MP-10 attenuates wire injury-induced intimal thickening *in vivo*

To examine the pharmacological effects of inhibiting PDE10A on intimal hyperplasia, we treated mice with MP-10 systemically. MP-10 has been tested in both clinical trials in treating schizophrenia[23,40] and Huntington's disease[24] and studies of cancer cell growth *in vitro*.[31,32] Only male mice were used in this study since we did not observe gender differences in PDE10A-mediated regulation of intimal thickening (*Figure 6B–G*). We pretreated animals with vehicle or MP-10 (10 mg/kg/day) subcutaneously 3 days before the surgery and continued the administration for 4 weeks (*Figure 7A*). This dose of MP-10 has established efficacy in mice in previously published studies.[40,41] We found that MP-10 treatment developed less neointima than the vehicle group. The quantitative results further revealed that intimal areas (*Figure 7B*) but not medial areas (*Figure 7C*) were reduced in the MP-10-treated group compared to the vehicle-treated group, and the ratio of intima/media was also reduced (*Figure 7D*). There was no significant difference in the EEL length between injured femoral arteries of vehicle- or MP-10-treated group (Supplementary material online, *Figure S7C*). The results from MP-10 are comparable with those from PDE10A-KO.

## 3.8 PDE10 inhibition attenuates human saphenous vein remodelling *ex vivo*

To further determine the role of PDE10A in human vascular remodelling, we used HSV samples. HSV is often used in CABG surgery for patients with coronary artery disease, though the risk of in-graft stenosis and graft failure increases gradually post-surgery.[3,11] When cultured *ex vivo*, HSV spontaneously undergoes remodelling, which represents a great system to test pharmacological reagents on human vessels.[42,43] After HSV segments were cultured *ex vivo* for 2 weeks, the thickness of intima and media was increased, and MP-10 treatment reduced the thickening of the vein wall (*Figure 7E*). We cultured HSV discards from 17 patients who underwent CABG surgery and found that remodelling and wall thickening of those HSV segments were significantly inhibited by MP-10 treatment (*Figure 7F–H*). PCNA, a cell proliferating marker, was found to be suppressed by MP-10 in cultured segments (*Figure 7I and J*). The results of individual vessel remodelling can be seen in Supplementary material online, *Figure S8*.

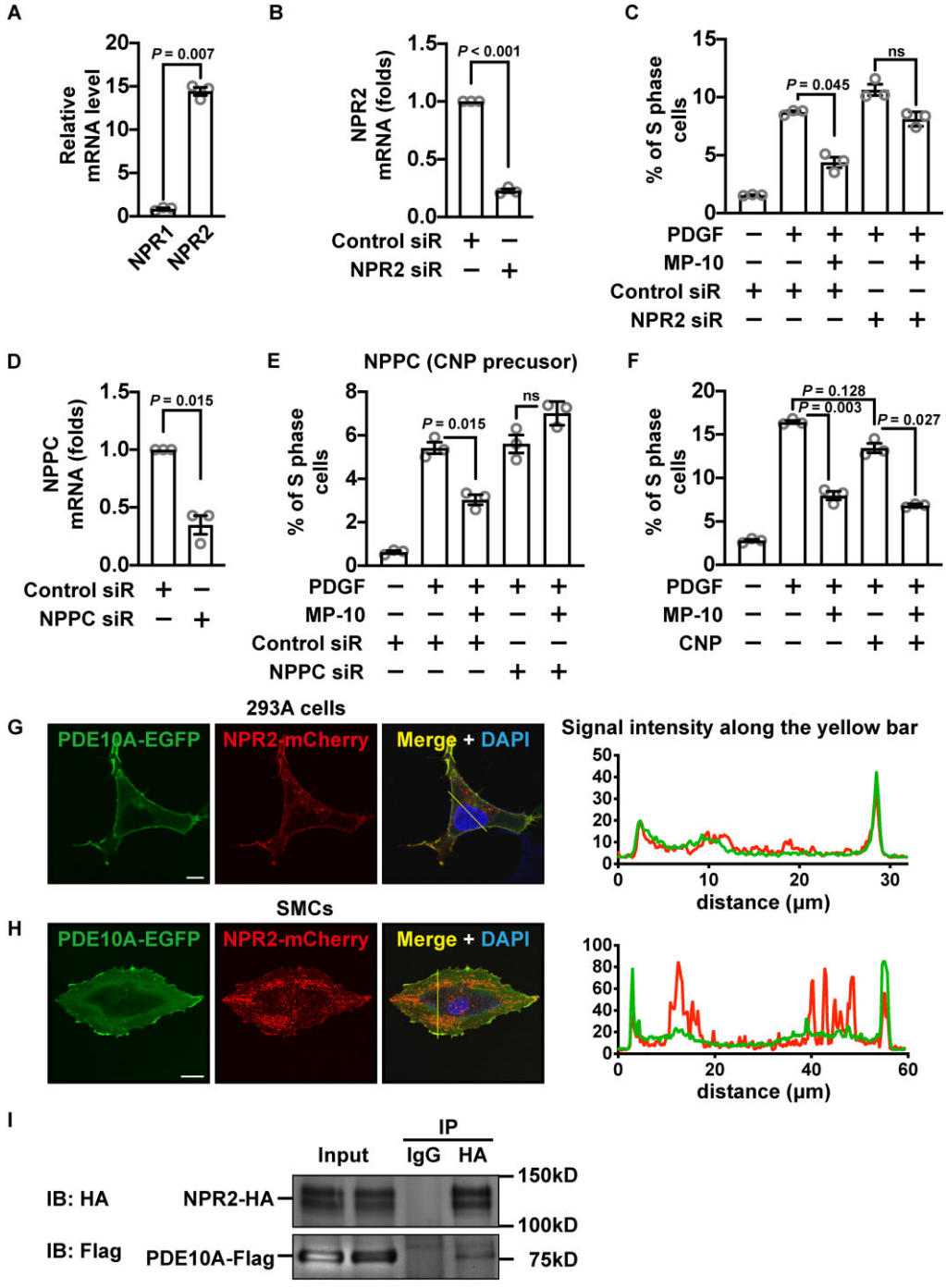


**Figure 5** PDE10A-modulated SMC proliferation is associated with CNP/NPR2 signalling pathway. (*A*) Relative mRNA levels of NPR1 and NPR2 in rat SMCs. An unpaired Student's *t*-test with Welch's correction was performed. $n = 3$ for each group. (*B*) RT-qPCR showing the level of NPR2 in SMCs treated with control or NPR2 siRNA. The expression level was normalized to the control siRNA-treated group. A one-sample *t*-test was performed to determine the knockdown efficiency. $n = 3$ for each group. (*C*) Percentages of S-phase cells treated with 2.5 μM MP-10, NPR2 siRNA, or both. A Welch's ANOVA with Dunnett's T3 multiple comparisons test was applied. $n = 3$ for each group. (*D*) RT-qPCR results showing the level of NPPC (encoding a precursor of CNP) in SMCs treated with control or NPRC siRNA. The mRNA level was normalized to the control siRNA-treated group. A one-sample *t*-test was performed to determine the knockdown efficiency. $n = 3$ for each group. (*E*) Percentages of S-phase cells treated with 2.5 μM MP-10, NPPC siRNA, or both. A Welch's ANOVA with Dunnett's T3 multiple comparisons test was applied. $n = 3$ for each group. (*F*) Percentages of rat SMCs in the S-phase after being treated with 2.5 μM MP-10, 1 μM CNP, or both. A Welch's ANOVA with Dunnett's T3 multiple comparisons test was performed. $n = 3$ for each group. (*G and H*) Confocal microscopic images (left panels) showing the signals of EGFP-tagged PDE10A (green) and mCherry-tagged NPR2 (red) overexpressed in 293A cells (*G*) or rat SMCs (*H*). Scale bar = 10μm (*G*) or 20 μm (*H*). The intensities of green and red signals across the cell were measured (right panels). (*I*) Immunoblot showing PDE10A and NPR2 from co-immunoprecipitation. Flag-tagged PDE10A and HA-tagged NPR2 were overexpressed in 293A cells. All data are shown as mean ± SEM. $n = 3$ for each group. ns, not significant.

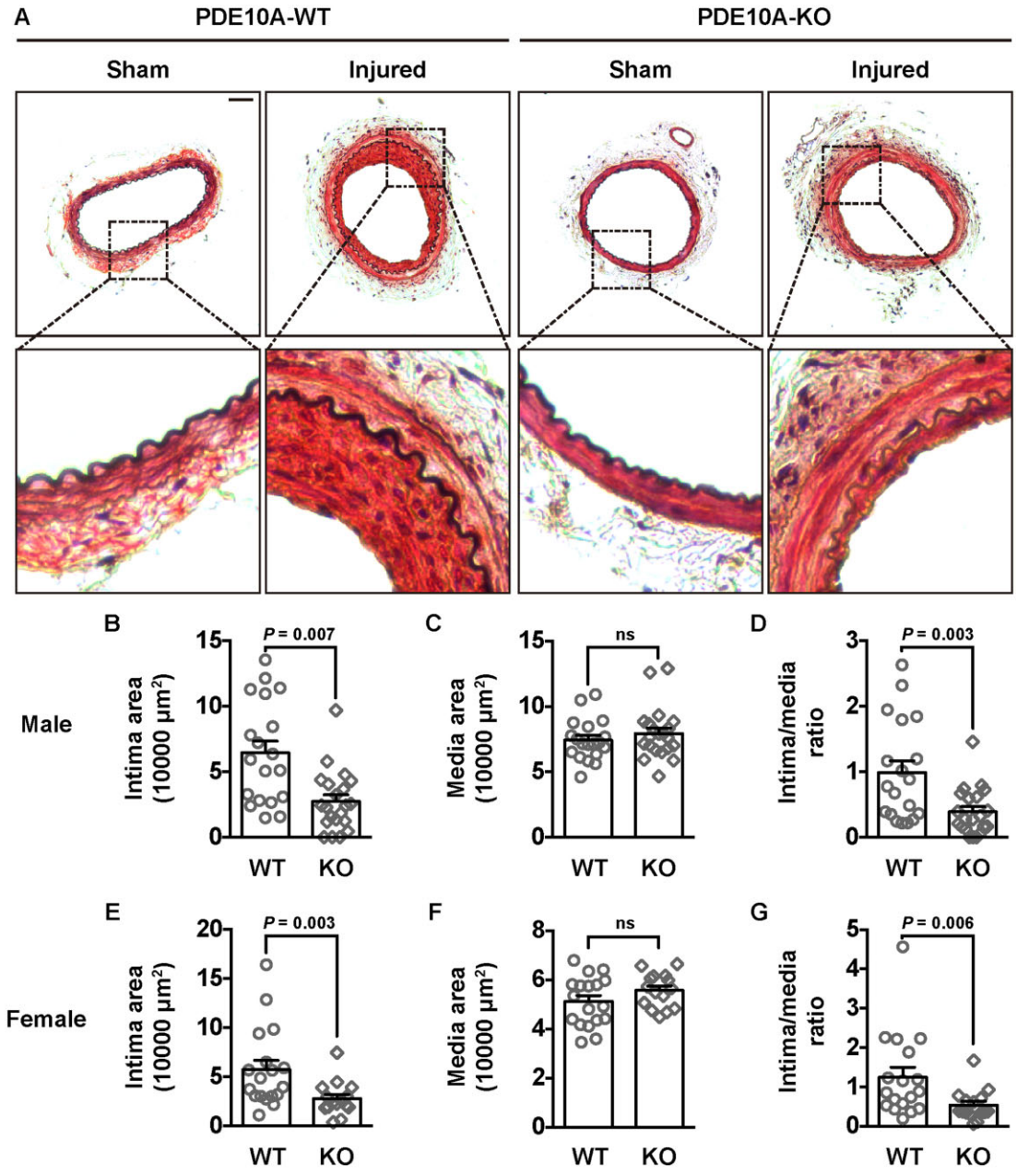


**Figure 6** Neointimal formation in femoral arteries of PDE10A-WT and PDE10A-KO mice after wire injury. (*A*) Representative histological images of cross-sections of femoral arteries from male WT and KO mice. The right femoral arteries were undergone wire injury and the left femoral arteries served as sham controls. Elastin in the internal and external laminae was stained black. (*B*) Intimal area, (*C*) medial area, and (*D*) the intima/media ratio of femoral arteries of male WT and KO mice. Five sections, 300 μm apart, were measured and averaged for each animal. An unpaired Student's *t*-test was used for comparing the intima area. Mann–Whitney tests were used for the medial area and the intima/media ratio. $n = 19$ mice for WT and $n = 21$ mice for KO. (*E*) Intimal area, (*F*) medial area, and (*G*) the intima/media ratio of femoral arteries of female WT and KO mice. An unpaired Student's *t*-test was used for comparing the media area. Mann–Whitney tests were used for the intima area and the intima versus media ratio. $n = 18$ mice for WT and $n = 15$ mice for KO. Scale bar = 50μm. All data are shown as mean ± SEM.

## 4. Discussion

In this study, we demonstrated PDE10A was up-regulated in both cultured SMCs and injured mouse arteries. We found inhibiting PDE10A led to decreased SMC proliferation and cell cycle arrest at G1-phase. Our data also showed that PDE10A at least partially controlled SMC growth by modulating the cGMP/PKG signalling pathway that is likely connected to CNP/NPR2. Importantly, both genetic depletion and pharmacological inhibition of PDE10A decreased wire injury-induced neointimal formation in mice. Moreover, PDE10A inhibition also attenuated the remodelling of HSV segments *ex vivo*. Therefore, our results indicate that PDE10A induction plays a causative role in SMC-like cell proliferation

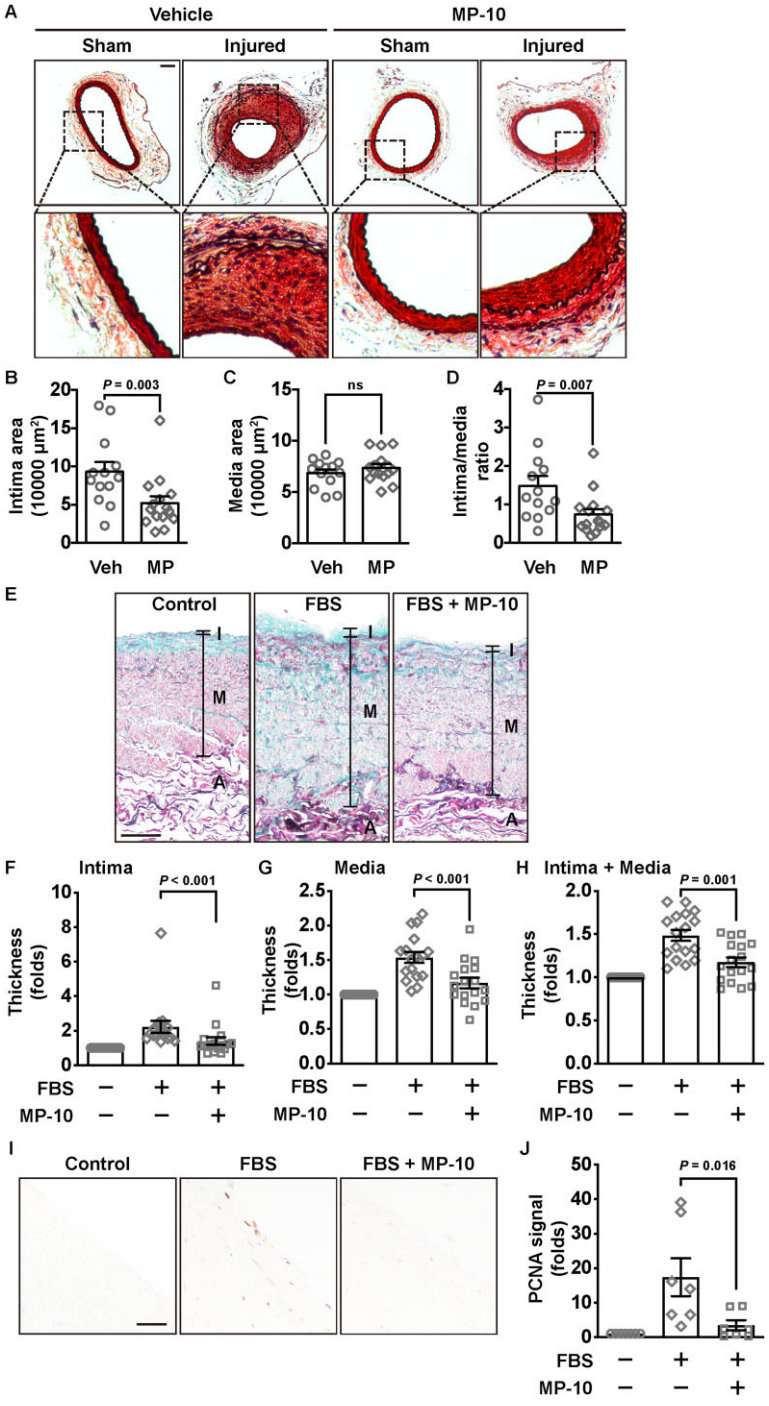


**Figure 7** Neointimal formation in wire-injured mouse femoral arteries and remodelling of HSV segments after vehicle or MP-10 treatment. (*A*) Representative histological images of cross-sections of sham and injured femoral arteries of control or MP-10-treated mice. Vehicle (40% HP-β-CD) or MP-10 (10 mg/kg/day) was administrated subcutaneously, which started 3 days before the surgery and lasted for 4 weeks. Scale bar = 50 μm. (*B*) Intimal area, (*C*) medial area, and (*D*) the intima/media ratio of mice 4 weeks after the surgery. An unpaired Student's *t*-test was used for comparing the media area. Mann–Whitney tests were used for the intima area and the intima/media ratio. $n = 13$ mice for vehicle treatment and $n = 15$ mice for MP-10 treatment. (*E*) Representative images showing HSV wall thicknesses from HSV segments without culture, or with culture in the presence of vehicle or MP-10 (20 μM). HSV segments were cultured in 15% FBS for 2 weeks. Samples were stained by the combined Verhoeff's elastic and Masson's trichrome method. Scale bar = 100μm. (*F–H*) The quantitative data showing thickness of the intimal layer (*F*), the medial layer (*G*), or the combined (intima + media) layer (*H*) of HSV samples from 17 patients after CABG. Thickness from three different locations of each section, and five sections, 500 μm apart, of each sample, were measured and averaged. The total thickness of both the intima and the media layers was calculated and normalized to the uncultured control group. Paired Student's *t*-tests were performed. (*I*) Immunohistochemical staining of PCNA in HSV samples. Scale bar = 50μm. (*J*) The quantitative data showing the fold change of the PCNA signal in HSV samples. Paired Student's *t*-tests were performed. $n = 7$ (randomly chosen from 17 patient samples). All data are shown as mean ± SEM.

and contributes to injury-induced intimal hyperplasia. Our study also suggests that PDE10A may represent a novel therapeutic target for vascular disorders associated with SMC overgrowth. It has long been believed that synthetic SMC-like cells in neointimal lesions are derived from the phenotypic modulation of medial SMCs. Recent lineage-tracing models have revealed that those synthetic SMCs may come from clonal expansion of progenitor-like cells,[44] including $SCA^+$ medial SMCs and $SCA^+GLI^+$ adventitial cells, which largely contribute to injury-induced intimal hyperplasia and atherosclerotic plaques in mouse models.[45–47] However, regardless of origins, our results suggest PDE10A in synthetic SMCs is critical in cell proliferation and neointima formation. Moreover, we are aware that the protective effects of PDE10A deficiency or inhibition on antagonizing intimal hyperplasia may not be exclusively contributed by SMCs. It is possible that PDE10A is expressed in other cell types of injured vessels, including but not limited to endothelial cells (ECs), fibroblast, and/or immune cells all of which are also important in vascular remodelling.[48,49] In addition, PDE10A in other tissues may modulate vascular remodelling indirectly. Therefore, cell-type-specific PDE10A deficient mice will be needed to further address the individual cellular contributions of PDE10A in vascular disorders.

Previous studies reported that PDE10A was highly expressed in tissues such as the brain and the testis.[28–30] PDE10A was not reported in vascular tissues due to the low expression level in healthy vessels. We found its expression was significantly enhanced in pathological vascular models. After the femoral artery wire injury, the greatest induction of PDE10A occurred in the intima area where synthetic SMCs are the predominant cell type. These results provided some evidence for cell and tissue-specificity of targeting PDE10A in vasculopathy without affecting normal vascular functions. PDE10A up-regulation in the diseased states has also been reported in a number of other peripheral tissues. For example, PDE10A was highly induced in mouse and human failing hearts, and inhibition of PDE10A was able to rescue cardiac hypertrophy and dysfunction.[33] PDE10A inhibition was also found to ameliorate pulmonary hypertension.[50] PDE10A was highly expressed in brown adipose tissue, and chronic inhibition in diet-induced obese mice was found to cause weight loss and improved insulin sensitivity.[51] In colon and lung tumour cells, PDE10A was also highly expressed, and its inhibition repressed cultured tumour cell growth.[31,32] Therefore, the expression and function of PDE10A deserve to be further investigated under different diseased states. How PDE10A is up-regulated in growing SMCs and injured vessels remains unclear. The PDE10A gene has a very large 1st intron (≈100 kb) and many human disease-associated PDE10A SNPs from genome-wide association studies are found in this intron, e.g. bipolar disorders,[52] executive functioning resilience,[53] conduct disorder,[54] asthma,[55] and hypothyroidism.[56,57] Bioinformatic analysis revealed many evolutionally conserved regions between humans and rodents in the intron (data not shown), suggesting the critical role of this intron in PDE10A gene regulation.

Several PDEs have been shown to regulate cGMP-mediated signalling in SMCs. For example, we have previously found that PDE1A, preferentially hydrolyzing cGMP, is predominantly cytoplasmic in medial contractile SMCs but is nuclear in synthetic SMCs of intimal lesions.[58] Cytoplasmic PDE1A regulates myosin light chain phosphorylation and promotes SMC contraction,[58] while nuclear PDE1A stimulates synthetic SMC growth and survival.[58,59] PDE1A is activated by $Ca^{2+}$/CaM,[60] which makes PDE1A important in $Ca^{2+}$-mediated regulation of cGMP.[61] However, the *in vivo* function of PDE1A in animal models of vascular remodelling remains to be explored. In the current study, our findings suggest that PDE10A regulates SMC proliferation by modulating cGMP/PKG signalling. However, their roles in SMC survival are different: PDE1A inhibition triggers SMC death,[44] while PDE10A inhibition does not have effects on SMC viability. The sources of cGMP that are regulated by PDE1A and PDE10A are likely different. PDE1A is localized in the nucleus of synthetic SMCs, suggesting its role in regulating nuclear cGMP signalling. However, PDE10A is anchored to the plasma membrane and coupled to CNP/NPR2. Another cGMP-PDE in SMCs is PDE5A. PDE5A is highly expressed in contractile SMCs and plays a critical role in negatively regulating NO/cGMP-mediated vasodilation.[62] PDE5 inhibition was also reported to inhibit SMC proliferation and attenuate pulmonary hypertension, and it has been shown to prevent neointimal formation in a rabbit carotid artery anastomosis model,[63] but it had no effects on intimal hyperplasia induced by carotid artery ligation surgery in mice.[64] These findings suggest that different cGMP-hydrolyzing PDEs with different enzymatic and regulatory properties as well as distinct subcellular localization and interacting molecules, thus play unique roles in vascular SMCs.

Our findings in the current study suggest that PKG1α and PKG1β exert different effects on SMC proliferation: PKG1α is anti-proliferative while PKG1β is pro-proliferative *in vitro*. Although the role and underlying mechanism of PKG1 in cGMP-mediated regulation of contractile SMC relaxation are well-established,[65] the roles of PKG1 in synthetic SMCs remain controversial. PKG1 has been shown to be down-regulated in synthetic SMCs compared to contractile SMCs.[65] Overexpressing a constitutively active catalytic domain of PKG1, which is shared by both PKG1α and PKG1β, reduced neointimal formation in balloon-injured rat carotid arteries, while overexpression of full-length PKG1β did not.[66] It has also been reported that SMC-specific knockout of PKG1 did not affect neointimal formation induced by ligation or endothelial denudation,[64] but contributed to the progress of atherosclerosis.[67] These discrepancies in the literature of PKG1 in different vascular disorders might be explained by the distinct functions of PKG1α and PKG1β in SMCs as well as contributions from other types of cells. The different functions of PKG1α or PKG1β in SMCs might result from their distinctive subcellular localizations and unique interacting protein partners due to their different N-terminal sequences. Thus, the precise roles of PKG1 need to be further investigated in an isozyme-specific manner.

In the striatum of a mouse brain, PDE10A inhibition has been shown to promote dopamine receptor-mediated cAMP/PKA signalling,[68,69] or nNOS/cGMP/PKG signalling.[70] In tumour cells, PDE10A inhibition has been shown to stimulate cGMP/PKG signalling, which antagonizes β-catenin-mediated transcription and promotes cancer cell apoptosis.[31] We failed to detect the effect of PDE10A inhibition on β-catenin signalling in SMCs (data not shown). We observed both increases in cAMP and cGMP levels in SMCs by PDE10A inhibition (*Figure 4A and B*). Our findings suggest that PDE10A-mediated regulation of CNP/NPR2/cGMP/PKG signalling plays a key role in PDE10A regulation of SMC proliferation. However, the role of cAMP elevation due to PDE10A inhibition remains unknown. Our result from the PKA blocker PKI does not support the role of PKA in PDE10A-mediated SMC proliferation (*Figure 4C*). In addition to PKA, the exchange protein directly activated by cAMP (Epac) is another cAMP effector. Previous studies have shown that Epac1 deficiency or pharmacological inhibition attenuated SMC proliferation or migration *in vitro* and suppressed neointimal formation *in vivo*.[71,72] These results suggest that Epac1 activation is associated with increased SMC growth and vascular hyperplasia, which does not support the contribution of Epac1 to the inhibitory effects of PDE10A inhibition/deficiency on SMC proliferation and vascular remodelling. There are two different Epac isozymes: Epac1 and 2. It remains unclear about the

differences between Epac1 and 2 in vascular SMCs. A previous study also reported that simultaneous activation of PKA and Epac (perhaps Epac1) elicited synergistic inhibitory effects on SMC proliferation *in vitro*,[73] suggesting a requirement for the activation of PKA and Epac by cAMP together. Nevertheless, the roles of PDE10A-mediated cAMP signalling in SMCs remain to be determined in the future.

It is known that the NO/sGC/cGMP/PKG signalling regulates contractile SMC contraction,[74] and there is also evidence that this signalling is anti-proliferative[75] and pro-apoptotic[76] in synthetic SMCs. However, we did not observe the involvement of sGCs in PDE10A-regulated SMC proliferation. It is well known that CNP, which is synthesized and released by ECs, binds and activates NPR2 on SMCs and thus inhibits cell proliferation.[77,78] However, CNP has also been found in SMCs, independent of the endothelium.[36,37] In fact, the level of CNP was increased in SMCs in the absence of ECs in injured vessels.[79] It seems CNP regulates SMC growth in both paracrine and autocrine manners, which explains that the addition of exogenous CNP only showed mild anti-mitogenic effects on cultured SMCs (*Figure 5F*). It was reported recently that male mice heterozygous for NPR2 depletion developed less neointima than WT mice after carotid artery ligation.[80] Therefore, it will be interesting to determine if an NPR2 agonist and a PDE10A inhibitor can have additive effects in suppressing intimal hyperplasia *in vivo*. Our co-immunostaining and co-immunoprecipitation studies indicate PDE10A and NPR2 can be spatially close on the plasma membrane. However, future studies are needed to further determine the endogenous protein interaction of these proteins *in vivo*.

# Supplementary material

Supplementary material is available at *Cardiovascular Research* online.

## Acknowledgements

The authors would like to thank Pfizer Inc. for sharing MP-10 (PF-2545920, Mardepodect).

**Conflict of interest:** V.A.K. received a research support LCZ696BUSNC16T from Novartis Pharmaceuticals Corp.

## Funding

This work was supported by the National Institute of Health (NIH) (R01HL134910 to C.Y. and B.C.B., R01HL154318 to C.Y.) and the American Heart Association (AHA) predoctoral fellowship (18PRE34030228 to L.L.).

## Data availability

The data underlying the findings of this study are available in the article and its supplementary material or from the corresponding author upon reasonable request.

## References

1. Liu MW, Roubin GS, King SB 3rd. Restenosis after coronary angioplasty. Potential biologic determinants and role of intimal hyperplasia. *Circulation* 1989;**79**:1374–1387.
2. Mintz GS, Popma JJ, Pichard AD, Kent KM, Satler LF, Wong C, Hong MK, Kovach JA, Leon MB. Arterial remodeling after coronary angioplasty: a serial intravascular ultrasound study. *Circulation* 1996;**94**:35–43.
3. Motwani JG, Topol EJ. Aortocoronary saphenous vein graft disease: pathogenesis, predisposition, and prevention. *Circulation* 1998;**97**:916–931.
4. Cizek SM, Bedri S, Talusan P, Silva N, Lee H, Stone JR. Risk factors for atherosclerosis and the development of preatherosclerotic intimal hyperplasia. *Cardiovasc Pathol* 2007;**16**:344–350.
5. Kijani S, Vazquez AM, Levin M, Boren J, Fogelstrand P. Intimal hyperplasia induced by vascular intervention causes lipoprotein retention and accelerated atherosclerosis. *Physiol Rep* 2017;**5**:e13334.
6. Herring BP, Hoggatt AM, Burlak C, Offermanns S. Previously differentiated medial vascular smooth muscle cells contribute to neointima formation following vascular injury. *Vasc Cell* 2014;**6**:21.
7. Gomez D, Owens GK. Smooth muscle cell phenotypic switching in atherosclerosis. *Cardiovasc Res* 2012;**95**:156–164.
8. Marx SO, Totary-Jain H, Marks AR. Vascular smooth muscle cell proliferation in restenosis. *Circ Cardiovasc Interv* 2011;**4**:104–111.
9. Kim YG, Oh IY, Kwon YW, Han JK, Yang HM, Park KW, Lee HY, Kang HJ, Koo BK, Kim HS. Mechanism of edge restenosis after drug-eluting stent implantation. Angulation at the edge and mechanical properties of the stent. *Circ J* 2013;**77**:2928–2935.
10. Sudhir K, Hermiller JB, Ferguson JM, Simonton CA. Risk factors for coronary drug-eluting stent thrombosis: influence of procedural, patient, lesion, and stent related factors and dual antiplatelet therapy. *ISRN Cardiol* 2013;**2013**:748736.
11. Collins MJ, Li X, Lv W, Yang C, Protack CD, Muto A, Jadlowiec CC, Shu C, Dardik A. Therapeutic strategies to combat neointimal hyperplasia in vascular grafts. *Expert Rev Cardiovasc Ther* 2012;**10**:635–647.
12. Frobert O, Lagerqvist B, Carlsson J, Lindback J, Stenestrand U, James SK. Differences in restenosis rate with different drug-eluting stents in patients with and without diabetes mellitus: a report from the SCAAR (Swedish Angiography and Angioplasty Registry). *J Am Coll Cardiol* 2009;**53**:1660–1667.
13. Polson JB, Strada SJ. Cyclic nucleotide phosphodiesterases and vascular smooth muscle. *Annu Rev Pharmacol Toxicol* 1996;**36**:403–427.
14. Hayashi S, Morishita R, Matsushita H, Nakagami H, Taniyama Y, Nakamura T, Aoki M, Yamamoto K, Higaki J, Ogihara T. Cyclic AMP inhibited proliferation of human aortic vascular smooth muscle cells, accompanied by induction of p53 and p21. *Hypertension* 2000;**35**:237–243.
15. Indolfi C, Avvedimento EV, Di Lorenzo E, Esposito G, Rapacciuolo A, Giuliano P, Grieco D, Cavuto L, Stingone AM, Ciullo I, Condorelli G, Chiariello M. Activation of cAMP-PKA signaling *in vivo* inhibits smooth muscle cell proliferation induced by vascular injury. *Nat Med* 1997;**3**:775–779.
16. Yu SM, Hung LM, Lin CC. cGMP-elevating agents suppress proliferation of vascular smooth muscle cells by inhibiting the activation of epidermal growth factor signaling pathway. *Circulation* 1997;**95**:1269–1277.
17. Wang S, Li Y. Expression of constitutively active cGMP-dependent protein kinase inhibits glucose-induced vascular smooth muscle cell proliferation. *Am J Physiol Heart Circ Physiol* 2009;**297**:H2075–H2083.
18. Cai Y, Nagel DJ, Zhou Q, Cygnar KD, Zhao H, Li F, Pi X, Knight PA, Yan C. Role of cAMP-phosphodiesterase 1C signaling in regulating growth factor receptor stability, vascular smooth muscle cell growth, migration, and neointimal hyperplasia. *Circ Res* 2015;**116**:1120–1132.
19. Kim MJ, Park KG, Lee KM, Kim HS, Kim SY, Kim CS, Lee SL, Chang YC, Park JY, Lee KU, Lee IK. Cilostazol inhibits vascular smooth muscle cell growth by downregulation of the transcription factor E2F. *Hypertension* 2005;**45**:552–556.
20. Souness JE, Hassall GA, Parrott DP. Inhibition of pig aortic smooth muscle cell DNA synthesis by selective type III and type IV cyclic AMP phosphodiesterase inhibitors. *Biochem Pharmacol* 1992;**44**:857–866.
21. Tantini B, Manes A, Fiumana E, Pignatti C, Guarnieri C, Zannoli R, Branzi A, Galie N. Antiproliferative effect of sildenafil on human pulmonary artery smooth muscle cells. *Basic Res Cardiol* 2005;**100**:131–138.
22. Maurice DH, Ke H, Ahmad F, Wang Y, Chung J, Manganiello VC. Advances in targeting cyclic nucleotide phosphodiesterases. *Nat Rev Drug Discov* 2014;**13**:290–314.
23. Raheem IT, Schreier JD, Fuerst J, Gantert L, Hostetler ED, Huszar S, Joshi A, Kandebo M, Kim SH, Li J, Ma B, McGaughey G, Sharma S, Shipe WD, Uslaner J, Vandeveer GH, Yan Y, Renger JJ, Smith SM, Coleman PJ, Cox CD. Discovery of pyrazolopyrimidine phosphodiesterase 10A inhibitors for the treatment of schizophrenia. *Bioorg Med Chem Lett* 2016;**26**:126–132.
24. McColgan P, Tabrizi SJ. Huntington's disease: a clinical review. *Eur J Neurol* 2018;**25**:24–34.
25. Garcia AM, Salado IG, Perez DI, Brea J, Morales-Garcia JA, Gonzalez-Garcia A, Cadavid MI, Loza MI, Luque FJ, Perez-Castillo A, Martinez A, Gil C. Pharmacological tools based on imidazole scaffold proved the utility of PDE10A inhibitors for Parkinson's disease. *Future Med Chem* 2017;**9**:731–748.
26. Leuti A, Laurenti D, Giampa C, Montagna E, Dato C, Anzilotti S, Melone MAB, Bernardi G, Fusco FR. Phosphodiesterase 10A (PDE10A) localization in the R6/2 mouse model of Huntington's disease. *Neurobiol Dis* 2013;**52**:104–116.
27. Seeger TF, Bartlett B, Coskran TM, Culp JS, James LC, Krull DL, Lanfear J, Ryan AM, Schmidt CJ, Strick CA, Varghese AH, Williams RD, Wylie PG, Menniti FS. Immunohistochemical localization of PDE10A in the rat brain. *Brain Res* 2003;**985**:113–126.
28. Fujishige K, Kotera J, Omori K. Striatum- and testis-specific phosphodiesterase PDE10A isolation and characterization of a rat PDE10A. *Eur J Biochem* 1999;**266**:1118–1127.

29. Soderling SH, Bayuga SJ, Beavo JA. Isolation and characterization of a dual-substrate phosphodiesterase gene family: PDE10A. *Proc Natl Acad Sci USA* 1999;**96**:7071–7076.
30. Fujishige K, Kotera J, Michibata H, Yuasa K, Takebayashi S, Okumura K, Omori K. Cloning and characterization of a novel human phosphodiesterase that hydrolyzes both cAMP and cGMP (PDE10A). *J Biol Chem* 1999;**274**:18438–18445.
31. Lee K, Lindsey AS, Li N, Gary B, Andrews J, Keeton AB, Piazza GA. beta-catenin nuclear translocation in colorectal cancer cells is suppressed by PDE10A inhibition, cGMP elevation, and activation of PKG. *Oncotarget* 2016;**7**:5353–5365.
32. Zhu B, Lindsey A, Li N, Lee K, Ramirez-Alcantara V, Canzoneri JC, Fajardo A, Madeira da Silva L, Thomas M, Piazza JT, Yet L, Eberhardt BT, Gurpinar E, Otali D, Grizzle W, Valiyaveettil J, Chen X, Keeton AB, Piazza GA. Phosphodiesterase 10A is overexpressed in lung tumor cells and inhibitors selectively suppress growth by blocking beta-catenin and MAPK signaling. *Oncotarget* 2017;**8**:69264–69280.
33. Chen S, Zhang Y, Lighthouse JK, Mickelsen DM, Wu J, Yao P, Small EM, Yan C. A novel role of cyclic nucleotide phosphodiesterase 10A in pathological cardiac remodeling and dysfunction. *Circulation* 2020;**141**:217–233.
34. Baldin V, Lukas J, Marcote MJ, Pagano M, Draetta G. Cyclin D1 is a nuclear protein required for cell cycle progression in G1. *Genes Dev* 1993;**7**:812–821.
35. Pohler D, Butt E, Meissner J, Muller S, Lohse M, Walter U, Lohmann SM, Jarchau T. Expression, purification, and characterization of the cGMP-dependent protein kinases I beta and II using the baculovirus system. *FEBS Lett* 1995;**374**:419–425.
36. Naruko T, Itoh A, Haze K, Ehara S, Fukushima H, Sugama Y, Shirai N, Ikura Y, Ohsawa M, Ueda M. C-Type natriuretic peptide and natriuretic peptide receptors are expressed by smooth muscle cells in the neointima after percutaneous coronary intervention. *Atherosclerosis* 2005;**181**:241–250.
37. Woodard GE, Rosado JA, Brown J. Expression and control of C-type natriuretic peptide in rat vascular smooth muscle cells. *Am J Physiol Regul Integr Comp Physiol* 2002;**282**:R156–R165.
38. Charych EI, Jiang LX, Lo F, Sullivan K, Brandon NJ. Interplay of palmitoylation and phosphorylation in the trafficking and localization of phosphodiesterase 10A: implications for the treatment of schizophrenia. *J Neurosci* 2010;**30**:9027–9037.
39. Siuciak JA, McCarthy SA, Chapin DS, Martin AN, Harms JF, Schmidt CJ. Behavioral characterization of mice deficient in the phosphodiesterase-10A (PDE10A) enzyme on a C57/Bl6N congenic background. *Neuropharmacology* 2008;**54**:417–427.
40. Verhoest PR, Chapin DS, Corman M, Fonseca K, Harms JF, Hou X, Marr ES, Menniti FS, Nelson F, O'Connor R, Pandit J, Proulx-Lafrance C, Schmidt AW, Schmidt CJ, Suiciak JA, Liras S. Discovery of a novel class of phosphodiesterase 10A inhibitors and identification of clinical candidate 2-[4-(1-methyl-4-pyridin-4-yl-1H-pyrazol-3-yl)-phenoxymethyl]-quinoline (PF-2545920) for the treatment of schizophrenia. *J Med Chem* 2009;**52**:5188–5196.
41. Wilson JM, Ogden AM, Loomis S, Gilmour G, Baucum AJ 2nd, Belecky-Adams TL, Merchant KM. Phosphodiesterase 10A inhibitor, MP-10 (PF-2545920), produces greater induction of c-Fos in dopamine D2 neurons than in D1 neurons in the neostriatum. *Neuropharmacology* 2015;**99**:379–386.
42. Soyombo AA, Angelini GD, Bryan AJ, Jasani B, Newby AC. Intimal proliferation in an organ culture of human saphenous vein. *Am J Pathol* 1990;**137**:1401–1410.
43. Angelini GD, Soyombo AA, Newby AC. Winner of the ESVS prize 1990. Smooth muscle cell proliferation in response to injury in an organ culture of human saphenous vein. *Eur J Vasc Surg* 1991;**5**:5–12.
44. Basatemur GL, Jorgensen HF, Clarke MCH, Bennett MR, Mallat Z. Vascular smooth muscle cells in atherosclerosis. *Nat Rev Cardiol* 2019;**16**:727–744.
45. Chappell J, Harman JL, Narasimhan VM, Yu HX, Foote K, Simons BD, Bennett MR, Jorgensen HF. Extensive proliferation of a subset of differentiated, yet plastic, medial vascular smooth muscle cells contributes to neointimal formation in mouse injury and atherosclerosis models. *Circ Res* 2016;**119**:1313–1323.
46. Jacobsen K, Lund MB, Shim J, Gunnersen S, Füchtbauer E-M, Kjolby M, Carramolino L, Bentzon JF. Diverse cellular architecture of atherosclerotic plaque derives from clonal expansion of a few medial SMCs. *JCI Insight* 2017;**2**:e95890.
47. Kramann R, Goettsch C, Wongboonsin J, Iwata H, Schneider RK, Kuppe C, Kaesler N, Chang-Panesso M, Machado FG, Gratwohl S, Madhurima K, Hutcheson JD, Jain S, Aikawa E, Humphreys BD. Adventitial MSC-like cells are progenitors of vascular smooth muscle cells and drive vascular calcification in chronic kidney disease. *Cell Stem Cell* 2016;**19**:628–642.
48. Behrendt D, Ganz P. Endothelial function. From vascular biology to clinical applications. *Am J Cardiol* 2002;**90**:40L–48L.
49. Danenberg HD, Fishbein I, Gao J, Monkkonen J, Reich R, Gati I, Moerman E, Golomb G. Macrophage depletion by clodronate-containing liposomes reduces neointimal formation after balloon injury in rats and rabbits. *Circulation* 2002;**106**:599–605.
50. Huang YY, Yu YF, Zhang C, Chen Y, Zhou Q, Li Z, Zhou S, Li Z, Guo L, Wu D, Wu Y, Luo HB. Validation of phosphodiesterase-10 as a novel target for pulmonary arterial hypertension via highly selective and subnanomolar inhibitors. *J Med Chem* 2019;**62**:3707–3721.
51. Hankir MK, Kranz M, Gnad T, Weiner J, Wagner S, Deuther-Conrad W, Bronisch F, Steinhoff K, Luthardt J, Kloting N, Hesse S, Seibyl JP, Sabri O, Heiker JT, Bluher M, Pfeifer A, Brust P, Fenske WK. A novel thermoregulatory role for PDE10A in mouse and human adipocytes. *EMBO Mol Med* 2016;**8**:796–812.
52. McDonald ML, MacMullen C, Liu DJ, Leal SM, Davis RL. Genetic association of cyclic AMP signaling genes with bipolar disorder. *Transl Psychiatry* 2012;**2**:e169.
53. Mukherjee S, Kim S, Ramanan VK, Gibbons LE, Nho K, Glymour MM, Ertekin-Taner N, Montine TJ, Saykin AJ, Crane PK; for the Alzheimer's Disease Neuroimaging Initiative. Gene-based GWAS and biological pathway analysis of the resilience of executive functioning. *Brain Imaging Behav* 2014;**8**:110–118.
54. Dick DM, Aliev F, Krueger RF, Edwards A, Agrawal A, Lynskey M, Lin P, Schuckit M, Hesselbrock V, Nurnberger J Jr, Almasy L, Porjesz B, Edenberg HJ, Bucholz K, Kramer J, Kuperman S, Bierut L; as part of the SAGE and GENEVA Consortia. Genome-wide association study of conduct disorder symptomatology. *Mol Psychiatry* 2011;**16**:800–808.
55. Melen E, Himes BE, Brehm JM, Boutaoui N, Klanderman BJ, Sylvia JS, Lasky-Su J. Analyses of shared genetic factors between asthma and obesity in children. *J Allergy Clin Immunol* 2010;**126**:631–637.e1–8.
56. Porcu E, Medici M, Pistis G, Volpato CB, Wilson SG, Cappola AR, Bos SD, Deelen J, den Heijer M, Freathy RM, Lahti J, Liu C, Lopez LM, Nolte IM, O'Connell JR, Tanaka T, Trompet S, Arnold A, Bandinelli S, Beekman M, Bohringer S, Brown SJ, Buckley BM, Camaschella C, de Craen AJ, Davies G, de Visser MC, Ford I, Forsen T, Frayling TM, Fugazzola L, Gogele M, Hattersley AT, Hermus AR, Hofman A, Houwing-Duistermaat JJ, Jensen RA, Kajantie E, Kloppenburg M, Lim EM, Masciullo C, Mariotti S, Minelli C, Mitchell BD, Nagaraja R, Netea-Maier RT, Palotie A, Persani L, Piras MG, Psaty BM, Raikkonen K, Richards JB, Rivadeneira F, Sala C, Sabra MM, Sattar N, Shields BM, Soranzo N, Starr JM, Stott DJ, Sweep FC, Usala G, van der Klauw MM, van Heemst D, van Mullem A, Vermeulen SH, Visser WE, Walsh JP, Westendorp RG, Widen E, Zhai G, Cucca F, Deary IJ, Eriksson JG, Ferrucci L, Fox CS, Jukema JW, Kiemeney LA, Pramstaller PP, Schlessinger D, Shuldiner AR, Slagboom EP, Uitterlinden AG, Vaidya B, Visser TJ, Wolffenbuttel BH, Meulenbelt I, Rotter JI, Spector TD, Hicks AA, Toniolo D, Sanna S, Peeters RP, Naitza S. A meta-analysis of thyroid-related traits reveals novel loci and gender-specific differences in the regulation of thyroid function. *PLoS Genet* 2013;**9**:e1003266.
57. Volpato CB, De Grandi A, Gogele M, Taliun D, Fuchsberger C, Facheris MF, Minelli C, Pattaro C, Pramstaller PP, Hicks AA. Linkage and association analysis of hyperthyrotropinaemia in an Alpine population reveal two novel loci on chromosomes 3q28-29 and 6q26-27. *J Med Genet* 2011;**48**:549–556.
58. Nagel DJ, Aizawa T, Jeon K-I, Liu W, Mohan A, Wei H, Miano JM, Florio V, Gao P, Korshunov V, Berk BC, Yan C. Role of nuclear Ca2+/calmodulin-stimulated phosphodiesterase 1A in vascular smooth muscle cell growth and survival. *Circ Res* 2006;**98**:777–784.
59. Jeon K-I, Jono H, Miller CL, Cai Y, Lim S, Liu X, Gao P, Abe J-I, Li J-D, Yan C. Ca2+/calmodulin-stimulated PDE1 regulates the beta-catenin/TCF signaling through PP2A B56 gamma subunit in proliferating vascular smooth muscle cells. *FEBS J* 2010;**277**:5026–5039.
60. Sonnenburg WK, Seger D, Beavo JA. Molecular cloning of a cDNA encoding the "61-kDa" calmodulin-stimulated cyclic nucleotide phosphodiesterase. Tissue-specific expression of structurally related isoforms. *J Biol Chem* 1993;**268**:645–652.
61. Yan C, Kim D, Aizawa T, Berk BC. Functional interplay between angiotensin II and nitric oxide: cyclic GMP as a key mediator. *Arterioscler Thromb Vasc Biol* 2003;**23**:26–36.
62. Clarke WR, Uezono S, Chambers A, Doepfner P. The type III phosphodiesterase inhibitor milrinone and type V PDE inhibitor dipyridamole individually and synergistically reduce elevated pulmonary vascular resistance. *Pulm Pharmacol* 1994;**7**:81–89.
63. Guzeloglu M, Aykut K, Albayrak G, Atmaca S, Oktar S, Bagriyanik A, Hazan E. Effect of tadalafil on neointimal hyperplasia in a rabbit carotid artery anastomosis model. *Ann Thorac Cardiovasc Surg* 2013;**19**:468–474.
64. Lukowski R, Weinmeister P, Bernhard D, Feil S, Gotthardt M, Herz J, Massberg S, Zernecke A, Weber C, Hofmann F, Feil R. Role of smooth muscle cGMP/cGKI signaling in murine vascular restenosis. *Arterioscler Thromb Vasc Biol* 2008;**28**:1244–1250.
65. Carvajal JA, Germain AM, Huidobro-Toro JP, Weiner CP. Molecular mechanism of cGMP-mediated smooth muscle relaxation. *J Cell Physiol* 2000;**184**:409–420.
66. Sinnaeve P, Chiche JD, Gillijns H, Van Pelt N, Wirthlin D, Van De Werf F, Collen D, Bloch KD, Janssens S. Overexpression of a constitutively active protein kinase G mutant reduces neointima formation and in-stent restenosis. *Circulation* 2002;**105**:2911–2916.
67. Wolfsgruber W, Feil S, Brummer S, Kuppinger O, Hofmann F, Feil R. A proatherogenic role for cGMP-dependent protein kinase in vascular smooth muscle cells. *Proc Natl Acad Sci USA* 2003;**100**:13519–13524.
68. Grauer SM, Pulito VL, Navarra RL, Kelly MP, Kelley C, Graf R, Langen B, Logue S, Brennan J, Jiang L, Charych E, Egerland U, Liu F, Marquis KL, Malamas M, Hage T, Comery TA, Brandon NJ. Phosphodiesterase 10A inhibitor activity in preclinical models of the positive, cognitive, and negative symptoms of schizophrenia. *J Pharmacol Exp Ther* 2009;**331**:574–590.
69. Polito M, Guiot E, Gangarossa G, Longueville S, Doulazmi M, Valjent E, Herve D, Girault JA, Paupardin-Tritsch D, Castro LR, Vincent P. Selective effects of PDE10A inhibitors on striatopallidal neurons require phosphatase inhibition by DARPP-32. *eNeuro* 2015;**2**:ENEURO.0060-15.2015.
70. Padovan-Neto FE, Sammut S, Chakroborty S, Dec AM, Threlfell S, Campbell PW, Mudrakola V, Harms JF, Schmidt CJ, West AR. Facilitation of corticostriatal transmission following pharmacological inhibition of striatal phosphodiesterase 10A: role of nitric oxide-soluble guanylyl cyclase-cGMP signaling pathways. *J Neurosci* 2015;**35**:5781–5791.
71. Kato Y, Yokoyama U, Yanai C, Ishige R, Kurotaki D, Umemura M, Fujita T, Kubota T, Okumura S, Sata M, Tamura T, Ishikawa Y. Epac1 deficiency attenuated vascular smooth muscle cell migration and neointimal formation. *Arterioscler Thromb Vasc Biol* 2015;**35**:2617–2625.

72. Wang H, Robichaux WG, Wang Z, Mei FC, Cai M, Du G, Chen J, Cheng X. Inhibition of Epac1 suppresses mitochondrial fission and reduces neointima formation induced by vascular injury. *Sci Rep* 2016;**6**:36552.
73. Hewer RC, Sala-Newby GB, Wu YJ, Newby AC, Bond M. PKA and Epac synergistically inhibit smooth muscle cell proliferation. *J Mol Cell Cardiol* 2011;**50**:87–98.
74. Nimmegeers S, Sips P, Buys E, Brouckaert P, Van de Voorde J. Functional role of the soluble guanylyl cyclase alpha(1) subunit in vascular smooth muscle relaxation. *Cardiovasc Res* 2007;**76**:149–159.
75. Tulis DA. Novel therapies for cyclic GMP control of vascular smooth muscle growth. *Am J Ther* 2008;**15**:551–564.
76. Pollman MJ, Yamada T, Horiuchi M, Gibbons GH. Vasoactive substances regulate vascular smooth muscle cell apoptosis. Countervailing influences of nitric oxide and angiotensin II. *Circ Res* 1996;**79**:748–756.
77. Hutchinson HG, Trindade PT, Cunanan DB, Wu CF, Pratt RE. Mechanisms of natriuretic-peptide-induced growth inhibition of vascular smooth muscle cells. *Cardiovasc Res* 1997;**35**:158–167.
78. Porter JG, Catalano R, McEnroe G, Lewicki JA, Protter AA. C-type natriuretic peptide inhibits growth factor-dependent DNA synthesis in smooth muscle cells. *Am J Physiol* 1992;**263**:C1001–C1006.
79. Brown J, Chen Q, Hong G. An autocrine system for C-type natriuretic peptide within rat carotid neointima during arterial repair. *Am J Physiol* 1997;**272**:H2919–H2931.
80. Korshunov VA, Smolock EM, Wines-Samuelson ME, Faiyaz A, Mickelsen DM, Quinn B, Pan C, Dugbartey GJ, Yan C, Doyley MM, Lusis AJ, Berk BC. Natriuretic peptide receptor 2 locus contributes to carotid remodeling. *J Am Heart Assoc* 2020;**9**:e014257.

## Translational perspective

Coronary artery disease is currently the leading cause of death worldwide. Smooth muscle cells (SMCs) are a major contributor to angioplasty restenosis, graft stenosis, and accelerated atherosclerosis. Current therapeutic approaches including drug-eluting stents targeting cell growth still have limitations. By combining studies on cultured SMCs *in vitro*, animal surgical models *in vivo*, and a human organ culture model *ex vivo*, we revealed an important role of PDE10A in modulating SMC proliferation and injury-induced intimal thickening. Given that PDE10A has been proven to be a safe drug target, its inhibition may represent a novel therapeutic strategy for vascular diseases associated with intimal hyperplasia.